

Research Article

Experimental and Theoretical Study of the Stability of the Complex Fisetin–Cu(II) and A Comparative Study of Free Ligand and Complex Interaction with Molecular Singlet Oxygen

Vanesa A. Muñoz¹, Frida C. D. Dimarco Palencia¹, Matias I. Sancho², Sandra Miskoski³, Norman A. García³, Gabriela V. Ferrari¹ and María Paulina Montaña^{1*} 

¹Facultad de Química, Bioquímica y Farmacia, Área de Química Física, Instituto de Química de San Luis INQUISAL (CONICET-UNSL), San Luis, Argentina

²Facultad de Química, Bioquímica y Farmacia, Área de Química Física, Instituto Multidisciplinario de Investigaciones Biológicas San Luis IMIBIO-SL (CONICET-UNSL), San Luis, Argentina

³Departamento de Química, Facultad de Ciencias Exactas Físico-Químicas y Naturales, Universidad Nacional de Río Cuarto, Río Cuarto, Argentina

Received 25 September 2019, accepted 19 December 2019, DOI: 10.1111/php.13213

ABSTRACT

In this work, the flavonol fisetin was selected in order to study its reactivity against Cu(II), a metal ion of interest in biological media and industry. The stoichiometry and apparent formation constant of the complex in ethanolic medium at 25°C were evaluated using spectrophotometric techniques. The resulting stoichiometry was a 1:1 ligand:metal complex, and a $\log K = 5.17 \pm 0.12$ was determined. Since two possible chelation sites can be proposed for the complex formation, quantum chemistry calculations were performed on these structures. Calculations suggest that the hydroxyl-keto site is more stable for the complex formation than the catechol site. Flavonoids could exert protection against oxidative damage caused by reactive oxygen species, and this biological activity could be affected by chelation with metal ions. This led us to perform a study on the interaction of both, free flavonoid and complex, with reactive oxygen species. Our results showed both compounds quench molecular singlet oxygen photogenerated with visible light, mainly in a physical fashion. In order to analyze a possible protective effect of flavonoid and its complex against oxidative damage in biological environments, the amino acid tryptophan was selected as a model oxidation system. Free flavonoid does not have a marked protective effect, whereas its complex showed a relevant protective effect.

Abbreviations: Fis, Fisetin; Fis-Cu(II), Fisetin–Cu(II) complex; Rf, riboflavin; RB, Rose Bengal; ROS, reactive oxygen species; FFAc, furfuryl acetate; SOD, superoxide dismutase; CAT, catalase; Trp, tryptophan.

INTRODUCTION

Several authors have reported flavonoids, secondary plant metabolites, as responsible of numerous biological properties: activity against viruses (1,2) and bacteria (3) as well as antiallergic (4), antithrombotic (5), anti-inflammatory (6) and antitumor

(7) activities. Their antioxidant activity (8) has also been studied, activity exerted by quenching (9,10) or by inhibiting the formation of reactive oxygen species (11,12). The fact that these compounds are able to complex metal ions (13,14) affects their biological activity (15–18) and is the reason why characterizing the formed complexes is a mandatory stage. The synthesis and characterization by means of spectroscopic data and thermal analysis of several metal–flavonoid complexes in solid state have been reported (18,19). However, data on flavonoid complexation ability in solution are minimal, one of the reasons for the relevance of this work.

Fisetin (3,7,3',4'-tetrahydroxyflavone) is a bioactive flavonol present in fruits and vegetables such as strawberries, apples, grapes and onions (20,21). The structure of this flavonol is shown in Fig. 1. Fisetin (Fis) exhibits several properties attributed to flavonoid family, such as antiviral (22), anticarcinogenic (23,24) and anti-inflammatory (20) activities, but also has other biological effects; for example, it stimulates signaling pathways that improve long-term memory (17). The antioxidant capacity of Fis has been studied in recent years, but there is not many

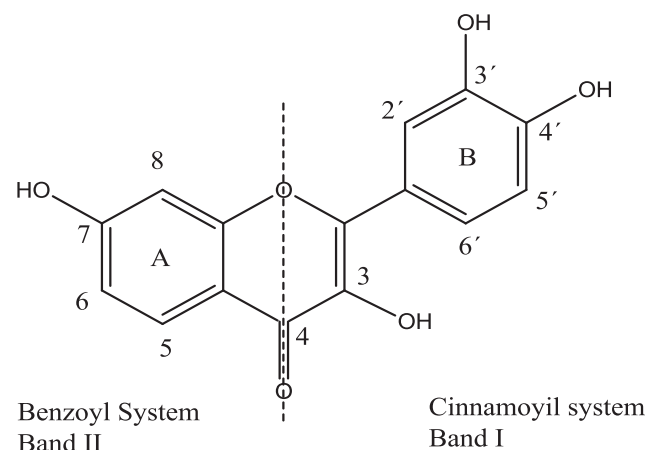


Figure 1. Structure of Fis and numbering of atoms.

*Corresponding author email: mpaulina.montana.a@gmail.com (M. Paulina Montaña)
© 2020 American Society for Photobiology

information about its activity in the presence of other compounds (25).

The flavonoids may form complexes with metal ions, and the number and position of their substituents affect the properties of the formed complexes as well as the type of coordination of metal ion (26–28). There are studies regarding the ability of Fis to complex metal ions; for example, Dimitrić Marković *et al.* (29), who studied the Fis-Al(III) complex, carried out theoretical and experimental studies that allowed determining the most important chelation sites in the ligand: the groups 3-hydroxy-4-carbonyl and 3',4'-dihydroxy. The study of the complexation of metal ions such as Cu(II), Fe(II) or Mn(II) by flavonoids continues to be of great scientific interest due to their role in living systems (30).

In this work, Cu(II) was selected as metal ion and its complexation with Fis was studied. Copper is a substance present in nature and plays an essential role in all living organisms. Some researchers have studied the effect of Cu(II) complexes with proteins and have observed a possible antioxidant capacity, finding a new perspective about copper complexes as antioxidants and possibly as therapeutic agents for neurodegenerative diseases (31).

Since complexation may change biological properties of Fis, a comparative study of free flavonoid and complex was carried out. The antioxidant activity of both compounds was studied, particularly the scavenging activity against molecular singlet oxygen ($O_2(^1\Delta_g)$). $O_2(^1\Delta_g)$ is a species which has attracted the attention of numerous researchers in last decades due to its physical, chemical and biological properties. Photosensitized production of $O_2(^1\Delta_g)$ is important in a wide range of areas from photodynamic cancer therapy (32) to polymer uses and its applications (33). Photosensitization uses the capacity of a given substance to absorb light radiation and generate electronically excited singlet and triplet states. The latter can react with molecular oxygen $O_2(^3\Sigma_g^-)$ and produce reactive oxygen species (ROS). $O_2(^1\Delta_g)$, superoxide radical anion ($O_2^{\cdot-}$), hydroxyl radical (HO^\cdot) and hydrogen peroxide (H_2O_2) constitute the so-called ROS which could act on biological targets present in the environment causing their oxidation (34). The presence of other substrates could exert a photoprotective effect deactivating these ROS.

In this work, the formation and stability of fisetin–Cu(II) complex were studied. The investigation involves the characterization of the complex using UV-Vis and FTIR techniques and a molecular modeling analysis to gain insight into the spectroscopic properties of the system. In addition, ability of free fisetin and the complex to deactivate ROS, mainly molecular singlet oxygen, through photosensitized processes was measured in a system that simulates a natural environment in the presence of visible light.

MATERIALS AND METHODS

Materials. Fisetin (CAS 528-48-3) was provided by Aldrich, while solutions of Cu(II) were prepared using $CuSO_4 \cdot 5H_2O$ p.a Merck (CAS 7758-99-8). The sensitizer riboflavin (CAS 83-88-5) was acquired from Aldrich, while Rose Bengal (CAS 11121-48-5) was purchased from Anedra. Furfuryl acetate (CAS 623-17-6) was acquired from Aldrich as well as the specific quenchers superoxide dismutase (CAS 9054-89-1) and catalase (CAS 9001-05-2), while L-tryptophan (CAS 73-22-3) was purchased from Sigma Chem. All these compounds were used as received. As solvent, ethanol HPLC quality (Sintorgan, CAS 64-17-5) was used and triply distilled water. In order to enlarge $O_2(^1\Delta_g)$ phosphorescence lifetime in time-resolved phosphorescence detection

(TRPD), deuterated water (D_2O , Aldrich, CAS 7789-20-0) and deuterated ethanol (EtOD, CAS 925-93-9) were employed (35). All experiments were made at room temperature and with freshly prepared solutions.

Spectrophotometric techniques. All UV-Vis spectra were recorded using an Agilent 8453 diode array spectrophotometer provided with an Agilent 89090A temperature controller and using 1 cm path length quartz cell with hermetical Teflon cover.

FTIR spectra of the free ligand and its complex were recorded in the 4000–400 cm^{-1} range with a 2 cm^{-1} spectral resolution using a Shimadzu IR Affinity-1. Spectrum of the complex was recorded after deposition of the sample solution on the surface of KBr pellets, a procedure successfully applied for flavonoid metallic complexes (36,37).

Stoichiometry and apparent formation constant. The determination of stoichiometry of fisetin–Cu(II) was taken using methods based on the spectrophotometric techniques. The continuous variation method, also known as Job's method, was used (38,39). This method requires the preparation of a set of solutions where the sum of total analytical concentration of Fis and Cu(II) is held constant while their ratio is varied. The absorbances of these solutions are measured at a wavelength where only the complex absorbs. A plot of mole fraction of ligand in the mixture vs. absorbance gives a triangular shaped curve. The legs of the triangle are extrapolated until they cross and the mole fraction at the point of intersection gives the stoichiometry of the complex.

This method allows determining the apparent formation constant, K , of the complex using the plot previously described and the following equation:

$$K = \frac{(A/(A_{\text{extp}})C)}{[M - (A/(A_{\text{extp}})C)][L - (A/(A_{\text{extp}})C)]} \quad (1)$$

where (A/A_{extp}) is the ratio between the measured and the extrapolated absorbances and C is the concentration of the metal or ligand, whichever is the limiting concentration at the intersection point.

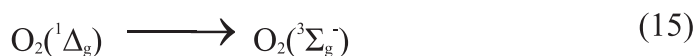
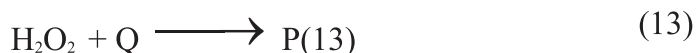
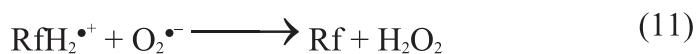
Computational details. The molecular geometry of Fis and the corresponding 1:1 Fis–Cu(II) complexes were fully optimized with the DFT functional UB3LYP (40,41) under an unrestricted scheme. The 6-31+G(d, p) basis set was employed for the H, C and O atoms, and for the Cu(II) ion, the Los Alamos double- ξ LANL2DZ effective core potential was implemented. A vibrational analysis was performed on the free flavonoid and the metallic complex in order to obtain thermodynamic parameters and to make sure that the calculated structures were true minima. The solvent effect on the gas-phase optimized structures was analyzed using the polarizable continuum model with the integral equation formalism (IEF-PCM) (42), and the UAHF radii set were employed to build the solvent cavity. A thermodynamic cycle was employed to estimate the Gibbs energy change in the complex formation (37). Nonequilibrium time-dependent density functional theory (TD-DFT) calculations were performed to estimate vertical excitation energies and absorption wavelengths of the complexes (43). Four functionals were tested in these calculations B3LYP (40), PBE0 (44,45), M06 (46) and CAM-B3LYP (47). Finally, the electronic transitions were analyzed using natural transition orbitals (NTOs) (48) which provides a good representation of the electronic transitions in terms of single particles. All the calculations were performed with the Gaussian 09 software package (49).

Stationary aerobic photolysis. Experiments employing sensitizers were carried out in a homemade photolyzer with filtered light from a 150-W quartz-halogen lamp. The sample was placed into a 1 cm path length cell, under magnetic stirring, and using cutoff filters at 480 nm. Under these conditions, neither Fis nor its complex absorbs any incident light.

The rate constant for the reaction $O_2(^1\Delta_g) + \text{Fis}$ or Fis-Cu(II) , k_t , (process (15), Scheme 12) was determined employing a previously described actinometric method (50). In this method, the slope of the first-order plot of oxygen consumption by Fis or Fis-Cu(II) (slope) and by a reference compound R (slope_R) are spectrophotometrically determined in the same experimental conditions. k_t of Fis or Fis-Cu(II) are calculated using the expression: $\text{slope/slope}_R = k_t/k_{tR}$. The reference used was FFAc, with a reported k_{tR} value of $7.8 \times 10^7 \text{ L mol}^{-1} \text{ s}^{-1}$ (51).

Rates of oxygen uptake (ROU) were determined employing a specific oxygen electrode Orion 810 A+, immersed in a 50 mL hermetically sealed Pyrex tube, which contained the sample solution. The system was irradiated with the above-described photolysis device.

Time-resolved $O_2(^1\Delta_g)$ Phosphorescence detection (TRPD). The rate constant k_t for overall quenching of $O_2(^1\Delta_g)$ by the flavonoid and its complex was determined employing time-resolved phosphorescence



Rate constant $k_t = k_r + k_q$

Scheme 1. Possible pathways in a Rf-photosensitized process in the presence of an electron donor transparent to the incident light (Q).

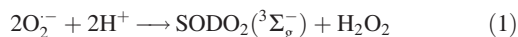
detection (TRPD) (52). The $\text{O}_2({}^1\Delta_g)$ emission at 1270 nm was generated by excitation of RB solutions at 532 nm with a Nd:YAG laser (Spectron), after filtering with a 1270-nm interference and a Wratten filter. At right angle, the phosphorescence signal was detected using an amplified Judson J16/8Sp Germanium detector. $\text{O}_2({}^1\Delta_g)$ phosphorescence lifetimes were evaluated in the absence (τ_0) and in the presence (τ) of the quencher (Fis or Fis-Cu(II)). The data were plotted according to a simple Stern-Volmer treatment: $\tau_0/\tau = 1 + k_t \tau_0$ [Fis or Fis-Cu(II)]. Aerated solutions were employed in all cases.

Quenching of Rf electronically excited states. The rate constant referred to the quenching of first electronically excited singlet state of Rf (${}^1\text{Rf}^*$) by Fis or its complex (1k_q , process (4)) was determined employing a classical Stern-Volmer treatment according to the expression $I_0/I = 1 + K_{sv}$ [Fis or Fis-Cu(II)], where I and I_0 are the respective stationary fluorescence intensities in the presence and in the absence of quencher. K_{sv} in the equation above is the Stern-Volmer constant ($K_{sv} = {}^1k_q \tau_0$) being ${}^1\tau_0 = 5$ ns, the Rf fluorescence lifetime (53). Fluorescence spectra were recorded using a FluoroMax 4 Horiba Jobin

Yvon spectrofluorimeter. The excitation and emission wavelengths employed were 445 and 517 nm, respectively.

The rate constant accounting for the quenching of electronically excited Rf (${}^3\text{Rf}^*$) by Fis or Fis-Cu(II) (3k_q , process (5)) could not be determined employing the conventional method of Laser Flash Photolysis (LFP) due to the overlapped ground state absorption bands of Rf and the quenchers at 337 nm, the available excitation wavelength in our LFP apparatus. Nevertheless, an alternative method was used to determine the rate constant considering that the anaerobic visible light-mediated degradation of Rf in solution occurs mainly from ${}^3\text{Rf}^*$ state, for which has a reported lifetime (${}^3\tau_0$) of 15 μs (54). The rate of the degradation process can be estimated through the time evolution of the absorbance decrease in the Rf absorption band at 445 nm. The decomposition rate of Rf was evaluated in the absence (V_0) and in the presence (V) of several Fis or Fis-Cu(II) concentrations, in N_2 saturated atmosphere. Employing the Stern-Volmer treatment ($V_0/V = 1 + {}^3k_q \text{ app } {}^3\tau_0 [\text{Fis or Fis-Cu(II)}]$), the apparent rate constant for the quenching of ${}^3\text{Rf}^*$ by Fis and Fis-Cu(II) was roughly evaluated. This indirect method allows to determine ${}^3k_q \text{ app}$ values with a $\pm 20\%$ error.

ROS deactivation. The possible photogeneration of ROS in solutions containing Rf and/or their possible deactivation caused by Fis or Fis-Cu(II) can be evaluated qualitatively through oxygen consumption in the presence of specific quenchers of ROS. In this work, three specific quenchers were used: sodium azide, a physical quencher of $\text{O}_2({}^1\Delta_g)$, superoxide dismutase, which dismutates $\text{O}_2^{\cdot-}$ (process (1)), and catalase, an enzyme responsible for the decomposition of H_2O_2 (process (2)) (55-57).



Photoprotection of tryptophan by Fis and Fis-Cu(II). Relative rates for Rf and RB sensitized photooxidation of the systems, Trp, Fis and Fis-Cu(II) and their mixtures were evaluated through the initial slope of oxygen consumption as a function of photoirradiation time, employing the specific oxygen electrode already described. Normalized rates for each sensitizer family were obtained as the quotient between the respective ROU for a given sample and that for the faster oxygen-consumer sample of the family. The experiments were carried out until 10–15% of oxygen consumption as a measure of the photooxidability of each studied system.

RESULTS

Complex stoichiometry and apparent constant formation determination

The absorption spectrum of Fis in ethanol medium is showed in Fig. 2. A shift to higher wavelength is observed when the metallic complex is formed. In order to study Fis-Cu(II) complex, solutions of different ligand:metal ratio were prepared. The spectra of these solutions were recorded and are shown in Fig. 2.

The stoichiometry of the complex was determined by Job's method, recording the spectra of a set of solutions where the ligand and metallic ion concentrations varied in the 1×10^{-4} – $1 \times 10^{-5} \text{ mol L}^{-1}$ range and total analytical concentration of Fis and Cu(II) was held constant at $1 \times 10^{-4} \text{ mol L}^{-1}$. Absorbances were measured at 475 nm, and a wavelength was only the complex absorbs. Data were used to build the graphic shown in Fig. 2 (inset), from which a 1:1 L:M stoichiometry was determined. A similar stoichiometry was reported for Fis-Al(III) complex at $\text{pH} \leq 5$ in aqueous media (29), while mono- and dinuclear species were reported for Fis-Cu(II) complexes in a 40:60 v/v methanol/water solvent (58).

The apparent formation constant of Fis-Cu(II) was determined in triplicate according to Job's method, previously described. The K values were obtained using Eq. (1) and data in Fig. 2. The log K value obtained at 25°C was 5.17 ± 0.12 . A value of

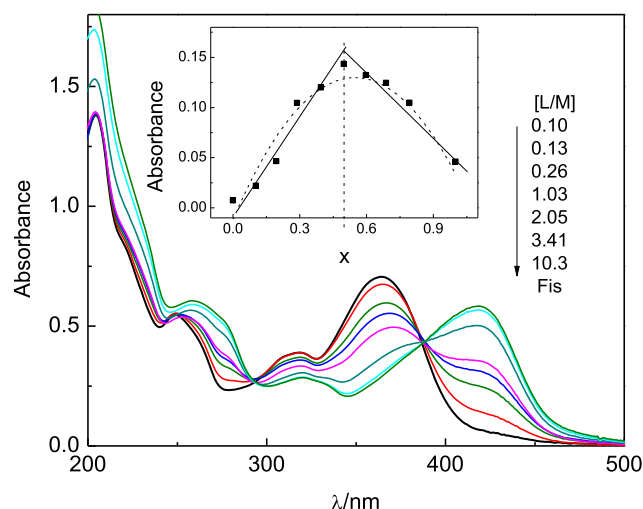


Figure 2. Spectra of Fis and its complex with Cu(II) in ethanolic media. Black spectrum corresponds to free ligand. Values between brackets correspond to different ligand:metal ratios. Inset: graphical representation of absorbance vs molar fraction (X) for Fis-Cu(II).

36.51 was reported for the overall stability constant of FisH_3^- and Cu(II) complex in a 40:60 v/v methanol/water solvent (42). Considering the ionization constant of FisH_3^- species reported in the same work, whose value is 29.87, the apparent formation constant of the complex is 6.64 ± 0.03 , slightly higher than the value obtained in this work in ethanol medium.

The formation constant of Fis-Cu(II) was also estimated by means of quantum chemistry calculations. Since Fis exhibits two possible chelating sites for Cu(II) ions, different structures were employed in the calculations. The first structure corresponds to the formation of a cationic complex where the chelation takes place in the 3-OH and 4-oxo site (i), and the second one is for a neutral complex where the chelation takes place in the catechol group (ii). The ΔG_s (Gibbs energy change in ethanol) were calculated for both complexes using a thermodynamic cycle (see Figure S1). This method has been successfully applied in the calculation of Gibbs energies for other flavonoid metallic complexes (37). For the site (i), complex a $\Delta G_s = -66.62 \text{ kJ mol}^{-1}$ (log $K = 11.67$) was obtained, while for the site (ii), complex $\Delta G_s = 16.04 \text{ kJ mol}^{-1}$ (log $K = -5.58$). These results indicate that the complexation Fis by Cu(II) is thermodynamically more stable when the metal interacts with the 3-OH-4-oxo site compared with the chelation in the catechol group. It is important to note that the interaction of Cu(II) with the 3-hydroxyl-4-oxo site involves the dissociation of one OH group of Fis, while the other chelation site (catechol) involves the dissociation of two OH groups. In addition, one of the complex has cationic nature, and the other is neutral (see Figure S1). The energy difference can be rationalized in terms of these features. Similar results were obtained by E. Jabeen *et al.* for the complexations of Cu(II) and Fe(III) with quercetin and morin (59). These authors reported negative ΔG values for the chelation site i and positive ΔG values for the chelation site ii using DFT calculations.

TD-DFT results

The optimized molecular structures of the Fis-Cu(II) are shown in Fig. 3. TD-DFT calculations were performed on complexes to

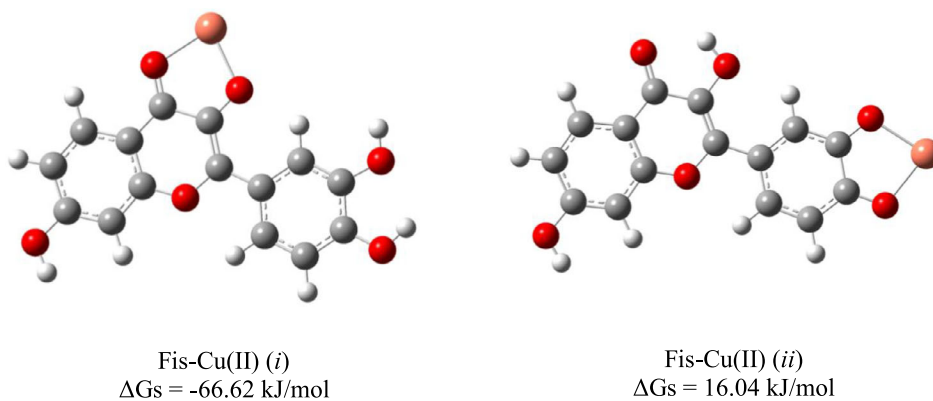


Figure 3. Optimized structures of Fis-Cu(II)(*i*) and Fis-Cu(II)(*ii*) calculated with the UB3LYP functional. ΔG_s is the Gibbs free energy of the complex formation in ethanolic solution.

Table 1. Calculated absorption wavelengths ($\lambda_{\text{TD-DFT}}$) in nm, oscillator strength (f) for the Fis-Cu(II) complexes from TD-DFT/PCM simulations. $\Delta\lambda$ is the difference between the calculated and experimental wavelengths in absolute value.

	B3LYP				PBE0		
	λ (exp)	λ TD-DFT	f	$\Delta\lambda$	λ TD-DFT	f	$\Delta\lambda$
Fis-Cu(II)(<i>i</i>)	429.6	491.2	0.3861	61.6	480.0	0.4400	50.44
Fis-Cu(II)(<i>ii</i>)	429.6	523.2	0.0682	93.6	522.3	0.1483	92.65

	M06				CAM-B3LYP		
	λ (exp)	λ TD-DFT	f	$\Delta\lambda$	λ TD-DFT	f	$\Delta\lambda$
Fis-Cu(II)(<i>i</i>)	429.6	487.3	0.3822	57.7	459.1	0.4478	29.5
Fis-Cu(II)(<i>ii</i>)	429.6	521.3	0.1280	91.7	495.7	0.3527	66.1

simulate the UV-Vis absorption spectra in ethanolic solution. For this purpose, the B3LYP, PBE0, M06 and CAM-B3LYP functionals were employed in combination with the IEF-PCM formalism. Table 1 shows the predicted absorption wavelengths ($\lambda_{\text{TD-DFT}}$) and oscillator strength (f) calculated for the two complexes. Taking into account the open-shell nature of the Fis-Cu(II) complex, spin contamination is observed in the TD-DFT results particularly in site (*ii*) complex. A measure of spin contamination is provided by the extent to which the calculated spin operator (\hat{S}^2) differs from the value expected from the same operator for a doublet state, which is 0.750 (60). Following an empirical rule, the absorption wavelengths reported in Table 1 have spin contaminations lower than 5% of the expected value ($\hat{S}^2 < 0.787$). According to these results, the predicted $\lambda_{\text{TD-DFT}}$ for the chelation site (*i*) are closer to the experimental values in comparison with the $\lambda_{\text{TD-DFT}}$ of the chelation site (*ii*). This trend is observed with the four functionals employed in the calculations, and the lowest $\Delta\lambda$ value (difference between experimental and calculated λ in absolute value) is obtained with the CAM-B3LYP functional (~29 nm). It is known that the preferential chelation site of

polyhydroxylated flavones depends on the experimental conditions. In this particular case, the TD-DFT calculations suggest that the 3-hydroxyl-4-oxo group is the most likely site for the chelation of Cu(II) ions.

To elucidate the nature of the electronic transitions of the Fis-Cu(II) complex UV-Vis spectrum, a natural transition orbital (NTO) analysis was performed. This approximation provides a compact representation of the transition density between the ground and excited states in terms of an expansion into single-particle transitions (47). These orbitals were constructed with the CAM-B3LYP functional since the most accurate $\lambda_{\text{TD-DFT}}$ value was obtained with this method. The NTOs of the Fis-Cu(II) complex are depicted in Fig. 4. Since these calculations are performed under an unrestricted scheme, the α and β spin orbitals are computed separately. For the *i*-Fis-Cu(II) complex, both spin orbitals have almost identical shape and energy for the analyzed transition. The adsorption band located at 429.6 nm ($\lambda_{\text{TD-DFT}} = 459.07$ nm) corresponds to $\pi-\pi^*$ transition, with a small contribution of a metal-to-ligand charge transfer (MLCT). The spin orbitals of the *ii*-Fis-Cu(II) complex have different shapes and energy, with a higher contribution of the β orbitals. The NTOs for the same absorption band calculated for *ii*-Fis-Cu(II) ($\lambda_{\text{TD-DFT}} = 495.70$ nm) show that this is mainly a $\pi-\pi^*$ transition-mixed metal-to-ligand charge transfer (MLCT).

FTIR results

The FTIR spectra of Fis and the metallic complex were recorded to evaluate the structural features of these compounds. The complexation with Cu(II) ions induces important changes in the fisetin spectra. The spectra of the free ligand and the complex are shown in Fig. 5. The sharp bands located at 1630 and 1606 cm^{-1} in Fis spectrum are assigned to the overlapping of the C=O and C2=C3 stretching modes (29). These are the most intense bands of Fis spectrum. In the 1500–1300 cm^{-1} range, the in-plane C-H bending and wagging vibrations can be found. The presence of vibration bands in the 3500–3200 cm^{-1} is attributed to the stretching vibrations of the many OH groups of the ligand. The bending vibrations of the different OH groups contribute to several modes located at 1440, 1340, 1183 and 1167 cm^{-1} (61). The formation of the metallic Fis-Cu(II) complex induces some important changes in the FTIR spectrum of the flavone. The C=O stretching vibration is shifted 10 cm^{-1} to

<i>i</i> -Fisetin-Cu(II)	Hole	Electron
T7(α) $\lambda_{\text{TD-DFT}} = 459.1 \text{ nm}$		
<i>ii</i> -Fisetin-Cu(II)		
T5(α) $\lambda_{\text{TD-DFT}} = 495.7 \text{ nm}$		
T5(β) $\lambda_{\text{TD-DFT}} = 495.7 \text{ nm}$		

Figure 4. Selected NTO plots representing the transitions of Fis-Cu(II) (i) and Fis-Cu(II) (ii) complexes calculated using the TD-CAM-UB3LYP method.

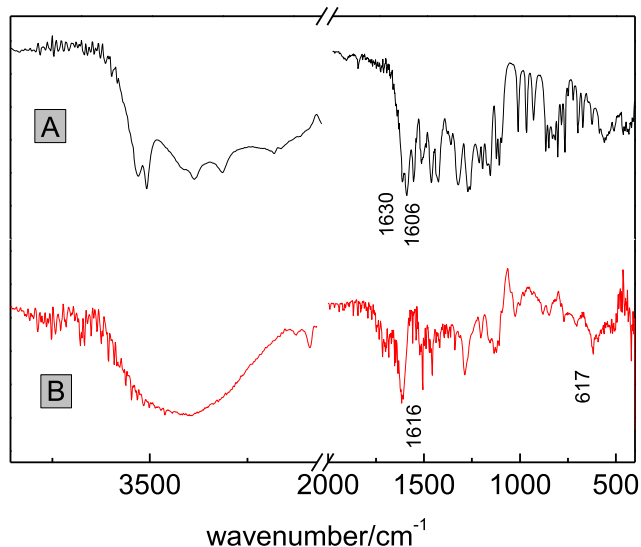


Figure 5. FTIR spectra of fisetin (A) and its Cu(II) complex (B). The frequency axis is broken between 2500 and 2000 cm^{-1} . No important bands have been observed in this region.

a higher wavenumber (1616 cm^{-1}), and a new band (weak) is observed at 617 cm^{-1} . This new band can be assigned to the Cu-O stretching vibration mode, which is consistent with previously reported wavenumbers for other Cu(II) complexes with flavonoids. In addition, there is an important reduction in the intensity (in relation to the most intense C=O vibration) of the bands located at 1340 , 1183 and 1167 cm^{-1} upon complexation. These results are not conclusive enough to elucidate the preferential chelation site of Fis-Cu(II) complex. However, they are indicative of a clear interaction between Cu(II) and fisetin and the formation of a metal complex.

Interaction of electronically excited states of Rf and Fis or Fis-Cu(II)

Flavonoids are involved in the generation and deactivation of oxidative specie (7,62). Study of photoprocesses in the presence of natural sensitizers can be used as an approach to real situations in living environments. Rf is a pigment considered as a possible sensitizer for photodegradation of natural substrates present in food and living organism (53). Since flavonoids and Rf are found in the same natural locations, information of the influence between this compounds will allow to gain insight into the behavior of this species in nature.

Rf in solution is able to photogenerate O_2^- (63) and $\text{O}_2(^1\Delta_g)$ (64), a behavior which may suffer variations in the presence of potential electron donors, as Fis or Fis-Cu(II). It is interesting then to study the interaction between this compounds and photoexcited Rf in order to determine whether Fis or Fis-Cu(II) is able to inhibit or favor the production of ROS.

Photoirradiation of Rf, Rf + Fis or Rf + Fis-Cu(II) in water: ethanol 70:30 v/v at wavelength where only the vitamin absorbs produces the spectral changes shown in Fig. 6.

Time evolution of the spectra indicates the occurrence of chemical changes involving the studied substrates and/or the photosensitizer. Even in the 450–500 nm range, there are spectral changes, a zone which clearly corresponds to Rf. These data definitively indicate electronically excited states of Rf, or the species produced from them with or without molecular oxygen participation are responsible for the observed changes.

A systematic kinetic study was carried out to evaluate and characterize the nature and mechanism of the possible processes involved in the sensitized degradation of Rf in the presence of Fis or Fis-Cu(II). Scheme 12 is used in order to discuss and evaluate the photophysical–photochemical results obtained from this study.

Scheme 12 shows a reaction sequence which includes photoprocesses in the presence and in the absence of a quencher (Q),

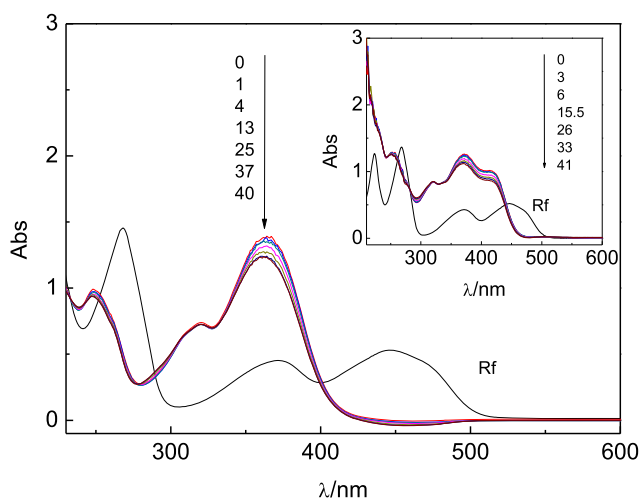


Figure 6. Spectral evolution of an aerated solution of 0.04 mmol L^{-1} Rf + 0.08 mmol L^{-1} Fis, in $\text{H}_2\text{O}/\text{EtOH}$ 70:30 v/v taken vs. 0.04 mM Rf, photoirradiated with 480 nm cutoff filter. Numbers next to the arrows represent time in minutes. Rf vs solvent spectrum is included for comparative purposes. Inset: spectral evolution of an aerated solution of 0.04 mmol L^{-1} Rf + 0.08 mmol L^{-1} Fis-Cu(II) in $\text{H}_2\text{O}/\text{EtOH}$ 70:30 v/v photoirradiated with 480 nm cutoff filter. Numbers next to the arrow represent time in minutes. Rf vs solvent spectrum is included for comparative purposes.

an electron donor transparent to the incident light, which in this case corresponds to Fis or Fis-Cu(II). P(n) are products for each corresponding (n) reaction, and $\text{O}_2(^3\Sigma_g^-)$ represents ground state molecular oxygen. Experimental conditions and nature of the involved compounds will determine the prevalence of a given photoprocess.

Interaction of Fis and Fis-Cu(II) with $\text{O}_2(^1\Delta_g)$

Both, flavonol and complex, were able to quench $\text{O}_2(^1\Delta_g)$. k_t values were obtained using TRPD, measuring the lifetime of $\text{O}_2(^1\Delta_g)$ generated from RB in a deuterated water:deuterated ethanol 70:30 v/v mixture according to techniques described before. In the presence of Fis or Fis-Cu(II), a decay in the phosphorescence of $\text{O}_2(^1\Delta_g)$ was observed, evidencing the interaction of these compounds with $\text{O}_2(^1\Delta_g)$. The phosphorescence lifetimes of $\text{O}_2(^1\Delta_g)$ measured were in agreement with those reported in the literature (35). Figure 7 (inset) shows obtained results, and Table 2 shows determined k_t values.

Rate constant k_t involves both physical deactivation and chemical deactivation of $\text{O}_2(^1\Delta_g)$. In order to discriminate the fraction of this deactivation involved in each of these processes, k_r values (process 15, Scheme 12) must be determined. This can be achieved measuring substrate consumption of solutions of Fis, Fis-Cu(II) and a reference (furfuryl acetate, FFAc) using water: EtOH 70:30 v/v as solvent and photogenerating $\text{O}_2(^1\Delta_g)$ from RB by photoirradiation employing a 480 nm cutoff filter. Data obtained are shown in Fig. 7, and k_r values are informed in Table 2.

A relatively easy way to evaluate the oxidability of substrates involves the calculation of the k_r/k_t ratio, a parameter which gives an approximate idea of the fraction of total quenching that leads to a chemical transformation. This parameter was calculated for both substrates, and values are informed in Table 2. The k_r/k_t values make evident two different behaviors: Fis

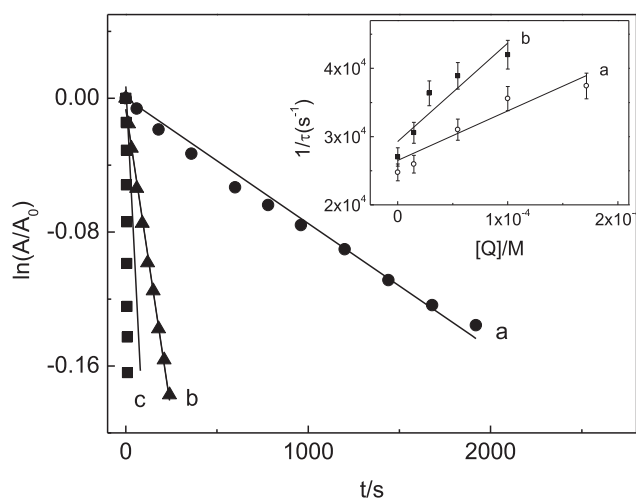


Figure 7. First-order representation for substrate consumption by photoirradiated ethanolic solutions of (a) RB ($A_{555} = 0.5$) + Fis ($7.8 \times 10^{-5} \text{ mol L}^{-1}$); (b) RB ($A_{555} = 0.5$) + Fis-Cu(II) ($7.8 \times 10^{-5} \text{ mol L}^{-1}$); (c) RB ($A_{555} = 0.5$) + FFAc ($8 \times 10^{-5} \text{ mol L}^{-1}$), in $\text{H}_2\text{O}:\text{EtOH}$ 70:30 v/v. Inset: Stern-Volmer treatment for the determination of the total rate constant for the quenching of $\text{O}_2(^1\Delta_g)$, k_t , by (a) Fis and (b) Fis-Cu(II) in $\text{D}_2\text{O}/\text{EtOH}$ 70:30 v/v.

interaction with $\text{O}_2(^1\Delta_g)$ is practically physical, a desirable characteristic for a ROS scavenger, while Fis-Cu(II) showed an important chemical contribution, almost equal to the physical contribution, a feature that distances it from being an ideal ROS scavenger. Other flavonoids and flavonoid complexes previously studied showed a different behavior compared with Fis and Fis-Cu(II). For instance, chrysin (5,7-dihydroxyflavone) has proven to be a sacrifice scavenger, and its interaction with $\text{O}_2(^1\Delta_g)$ is basically a chemical interaction ($k_r/k_t \sim 1$), while its Cu(II) complex showed a small chemical contribution ($k_r/k_t \sim 0.17$), making evident that $\text{O}_2(^1\Delta_g)$ scavenging ability was improved with complexation (65). A different case is presented by 3,3'-dihydroxyflavone and its La(III) complex: the calculated k_r/k_t ratios for the flavonoid and for the complex were, respectively, ~ 0 and 0.1 , indicating both compounds interact in a similar way with $\text{O}_2(^1\Delta_g)$ (66). These results make evident that to predict whether a given flavonoid complex will improve or decrease the chemical contribution of the $\text{O}_2(^1\Delta_g)$ interaction compared with the free ligand is not simple.

Quenching of Rf electronically excited states

Rf fluorescence spectrum shows a band centered at 517 nm when excited at 445 nm, with a quantum yield of 0.25 (53). In the presence of increasing concentrations of free flavonoid or complex, a decrease in the fluorescence intensity of the band is observed (see Supporting Information), evidencing the interaction with $^1\text{Rf}^*$ (process 4, Scheme 12). Fis and Fis-Cu(II) can interact with $^1\text{Rf}^*$ with 1k_q values $\sim 10^9 \text{ L mol}^{-1} \text{ s}^{-1}$. These high constant values imply the process 4 from the Scheme 12 does not operate in these systems due to the concentrations required to efficiently deactivate the vitamin excited state are much higher than those used in this work. A similar argument can be used to analyze the effect of Cu(II) ($^1k_q = 1.2 \times 10^9 \text{ L mol}^{-1} \text{ s}^{-1}$) (67), considering the concentration of free metallic ion in the medium

Table 2. Rate constant values for total (k_t) and reactive quenching (k_r) of $O_2(^1\Delta_g)$, k_r/k_t and quenching of $^3Rf^*$ (3k_q) values for Fis and Fis-Cu(II).

Compound	k_t (10^7 L mol $^{-1}$ s $^{-1}$)	k_r (10^6 L mol $^{-1}$ s $^{-1}$)	k_r/k_t	3k_q (10^7 L mol $^{-1}$ s $^{-1}$)
Fis	14.4	2.6	0.02	1.42
Fis-Cu(II)	7.25	26.6	0.36	1.38

calculated from the apparent stability constant of the complex is ~ 0.6 $\mu\text{mol L}^{-1}$, not enough to effectively quench $^1Rf^*$.

Fis and Fis-Cu(II) also interact with $^3Rf^*$, effect that is inferred from the decrease in the anaerobic photodecomposition of Rf when Fis or Fis-Cu(II) concentrations increase (Figs. 8 or 9). The $^3k_{q\text{-app}}$ values (process 7, Scheme 12) can be determined monitoring the 445 nm absorption band of oxygen-free solutions of Rf in ethanolic medium, irradiated in the absence and in the presence of different concentrations of free flavonoid or complex (Table 2). Both studied compounds exhibit high $^3Rf^*$ deactivation constant values, which means stationary concentration of $O_2(^1\Delta_g)$ could be diminished through this via, and in consequence, have a protective effect against this species.

Fis and Fis-Cu(II) as ROS scavengers

Oxygen consumption experiments in the presence and in the absence of specific ROS quenchers allowed to evaluate the

possible deactivation of ROS photogenerated from Rf + Fis or Rf + Fis-Cu(II) systems. The specific ROS quenchers used were as follows: NaN_3 , a physical quencher of $O_2(^1\Delta_g)$, SOD, which catalyzes dismutation of O_2^- , and CAT, which catalyzes the decomposition of H_2O_2 . Although $O_2(^1\Delta_g)$ is reactive toward proteins, employing the concentrations described in these experiments, the lifetime of this species is not affected. Moreover, all experiments were carried out keeping the concentrations of Rf and the corresponding substrate constant. The oxygen consumption profiles obtained by irradiating the above-described solutions were compared (Fig. 10).

In the presence of NaN_3 , no inhibition effect was observed (data not shown), while Fig. 10 shows oxygen uptake profiles for Rf + (free flavonoid or complex) and Rf + (free flavonoid or complex) in the presence of quenchers CAT and SOD. The first set of experiments involves Rf + Fis system and shows that the higher inhibition in the rate of oxygen consumption occurs in the presence of CAT. This inhibition indicates a reaction between Fis and H_2O_2

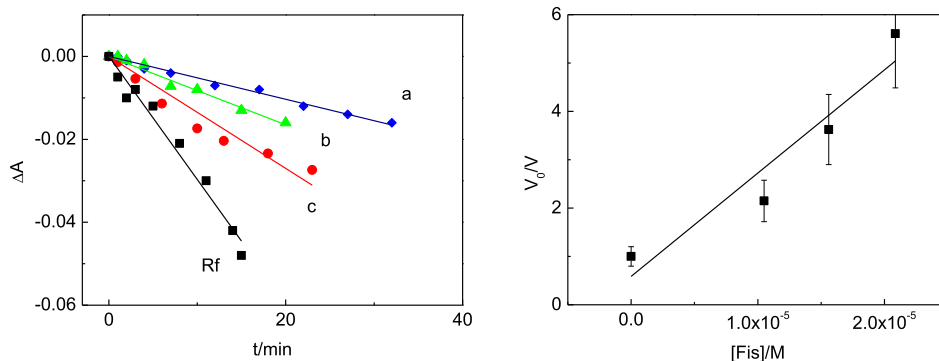


Figure 8. Left: Degradation of Rf as a function of photoirradiation time (cutoff 480 nm), monitored through the decrease in the 445 nm absorbance peak, in the absence (Rf) and in the presence of Fis: (a) 20.8 $\mu\text{mol L}^{-1}$; (b) 15.6 $\mu\text{mol L}^{-1}$ and (c) 15.6 $\mu\text{mol L}^{-1}$. Right: Stern-Volmer treatment for the evaluation of the rate constant for the quenching of $^3Rf^*$ by Fis in $\text{H}_2\text{O}:\text{EtOH}$ 70:30 v/v deaerated solutions. V_0 and V represent the respective rates of Rf degradation, upon photoirradiation (cutoff 480 nm), in the absence and in the presence of Fis.

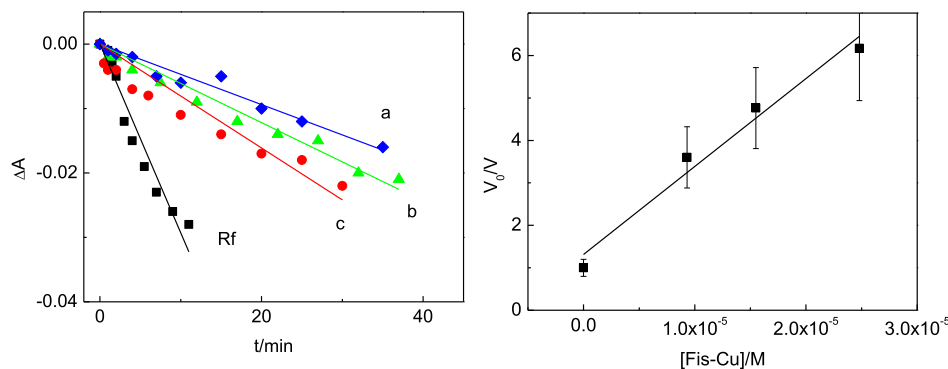


Figure 9. Left: Degradation of Rf as a function of photoirradiation time (cutoff 480 nm), monitored through the decrease in the 445 nm absorbance peak, in the absence (Rf) and in the presence of Fis-Cu(II): (a) 24.8 $\mu\text{mol L}^{-1}$, (b) 15.5 $\mu\text{mol L}^{-1}$ and (c) 9.3 $\mu\text{mol L}^{-1}$. Right: Stern-Volmer treatment for the evaluation of the rate constant for the quenching of $^3Rf^*$ by Fis-Cu(II) in $\text{H}_2\text{O}:\text{EtOH}$ 70:30 v/v deaerated solutions. V_0 and V represent the respective rates of Rf degradation, upon photoirradiation (cutoff 480 nm), in the absence and in the presence of Fis-Cu(II).

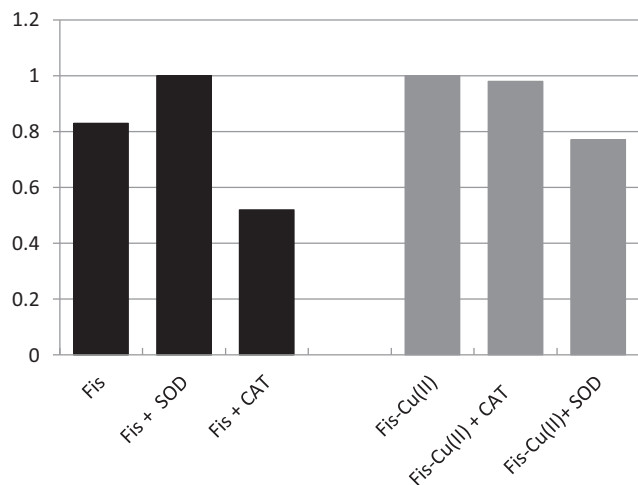


Figure 10. Normalized rate of oxygen uptake of aerated solutions of 0.04 mmol L^{-1} Rf + 0.05 mmol L^{-1} Fis or Rf + 0.05 mmol L^{-1} Fis-Cu(II) in the presence of the specific ROS quenchers: $1 \mu\text{g/mL}$ CAT, $1 \mu\text{g/mL}$ SOD. Solvent: $\text{H}_2\text{O}/\text{EtOH}$ 70:30 v/v.

generated from Rf (step 11, Scheme 12) could be occurring. In the presence of the inhibitor, H_2O_2 is deactivated and oxygen consumption decreases. In contrast, the rate of oxygen consumption is relatively increased in the presence of SOD compared to Rf + Fis. This corroborates the importance of the reaction between Fis and H_2O_2 since the hydrogen peroxide released during deactivation of O_2^- by SOD (Eq. 1) increases the oxygen uptake, minimizing participation of O_2^- in the reactive circuit.

Regarding the results obtained for Rf + Fis-Cu(II) in the presence of CAT, no effect was observed, which leads us to discard the contribution of H_2O_2 , considering same argument used before. The mixture Rf + Fis-Cu(II) + SOD shows a clear inhibition of the oxygen uptake and, hence, participation of O_2^- in the oxidative process.

Fis and Fis-Cu(II) as photoprotectors of tryptophan against photogenerated ROS

In order to analyze the possible protection effect in biological environments of the flavonoid and its complex with Cu(II) against oxidative damage, a model of oxidation of tryptophan (Trp) photosensitized with Rf was selected. Trp was chosen because it is an oxidizable amino acid involved in photodynamic processes of proteins (68). Trp interacts with $^3\text{Rf}^*$ with a 3k_q constant rate value of $2.5 \times 10^9 \text{ L mol}^{-1} \text{ s}^{-1}$ (69), and it interacts with $\text{O}_2(^1\Delta_g)$ with a $k_t = 7.2 \times 10^7 \text{ L mol}^{-1} \text{ s}^{-1}$ and $k_r = 4.7 \times 10^7 \text{ L mol}^{-1} \text{ s}^{-1}$ (67,70).

Kinetic information obtained measuring ROU provides a path to understand the protection exerted by flavonoids or their complexes on protein residues through photopromoted oxidation. The same experiments using RB instead of Rf as sensitizer facilitate interpretation on the grounds of an $\text{O}_2(^1\Delta_g)$ -mediated operation. Results are shown in Fig. 11.

As shown in Fig. 11, the photooxidation rate of the mixture Fis + Trp is lower than the sum of the photooxidation rates of Fis and Trp individually. This value added to the ability of Fis to deactivate $\text{O}_2(^1\Delta_g)$ through a physical mechanism and leads us to the conclusion that the flavonoid is able to protect Trp from the oxidative species. On the other hand, Trp + Fis-Cu(II)

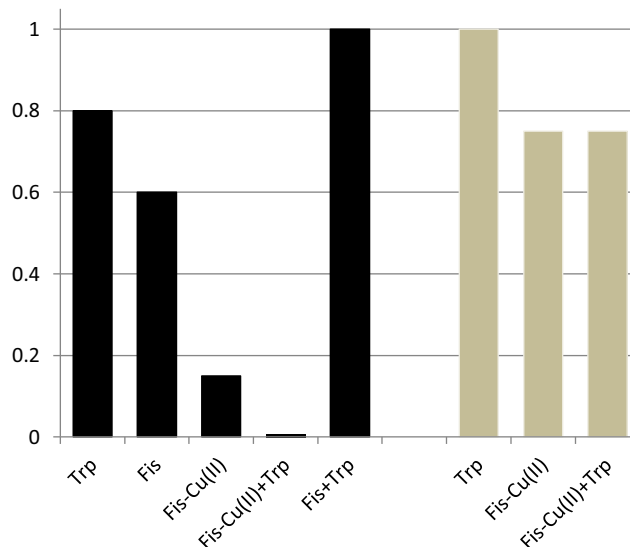


Figure 11. Rate of oxygen uptake of aerated solutions of Rf 0.04 mmol L^{-1} in the presence of Trp and/or Fis or Fis-Cu(II) (black bars). Rate of oxygen uptake of aerated solutions of RB ($A_{549\text{nm}} = 0.5$) in the presence of Trp, Fis-Cu(II) and Trp + Fis-Cu(II) (gray bars). All experiences were carried out irradiating using 480 nm filter. Solvent: $\text{H}_2\text{O}/\text{EtOH}$ 70:30 v/v. $[\text{Trp}] = [\text{Fis}] = [\text{Fis-Cu(II)}] = 0.05 \text{ mmol L}^{-1}$. [Color figure can be viewed at wileyonlinelibrary.com]

system shows practically no oxygen consumption, which implies a significant protection effect, even though the k_r/k_t ratio has a reactive component. In order to gain insight into this reaction, a new experiment was carried out measuring rate of oxygen uptake of similar solutions of Trp, Fis-Cu(II) and Trp + Fis-Cu(II) but replacing Rf by RB, which photogenerates $\text{O}_2(^1\Delta_g)$ exclusively. The results show the protective effect against $\text{O}_2(^1\Delta_g)$ exerted by the complex toward the amino acid is not enough to justify the behavior in the presence of Rf; hence, the protection exerted by the complex may include other reactive oxygen species.

CONCLUSIONS

In this work, the complex fisetin-Cu(II) was studied. The stoichiometry and apparent constant of Fis-Cu(II) complex were evaluated in $\text{H}_2\text{O}/\text{EtOH}$ 70:30 v/v solvent, resulting in a 1:1 ligand:metal complex stoichiometry with a $\log K = 5.17 \pm 0.12$ at 25°C . The molecular structure of the complex was analyzed by molecular modeling and FTIR analysis. Two possible chelation sites were proposed for the complex; the catechol group (site ii) is the preferred site of Cu(II) ions under the adopted conditions. However, these results suggest that the coexistence of both chelation sites must be considered.

Fisetin and its Cu(II) complex in ethanolic medium deactivate $\text{O}_2(^1\Delta_g)$ generated by visible light photosensitization, with an increased reactive component for the latter. The oxygen uptake profiles of the substrates in the presence of specific inhibitors of ROS indicate an interaction between Fis-Cu(II) and O_2^- . It is also possible to infer the participation of H_2O_2 in the photooxidative process in the presence of Fis. A model oxidation system was employed with Rf as photosensitizer and the amino acid tryptophan. Although free flavonoid has a protective effect, the protection exerted by complex is greater, evidencing an improvement of this capacity when complexation occurs.

FUNDING

This work was developed thanks to contributions from Consejo Nacional de Investigaciones Científicas y Técnicas (CONICET, PIP 11220170100208CO) and Secretarías de Ciencia y Técnica, Universidad Nacional de San Luis (SECyT UNSL, PROICO 2-3218- 22Q/809) and Universidad Nacional de Río Cuarto (SECyT UNRC), all in Argentine.

Authors appreciate language revision by staff from Instituto de Lenguas, UNSL.

SUPPORTING INFORMATION

Additional supporting information may be found online in the Supporting Information section at the end of the article:

Figure S1. Thermodynamic cycle employed for the calculation of the Gibbs energy change of the complex formation reaction. The first cycle correspond to the site (i) Fis-Cu complex and the second one to the site (ii) Fis-Cu complex.

Figure S2. Stern-Volmer treatment for the evaluation of the rate constant for the quenching of $1Rf^*$ by Fis (left) and Fis-Cu (II) (right) in $H_2O:EtOH$ 70:30 v/v. Insets: Fluorescence spectra of Rf in the presence of increasing concentration of Fis (left) and Fis-Cu(II) (right).

REFERENCES

- Casano, G., A. Dumètre, C. Pannecouque, S. Hutter, N. Azas and M. Robin (2010) Anti-HIV and antiparasitoid activity of original flavonoid derivatives. *Bioorg. Med. Chem.* **18**, 6012–6023.
- Sithisarn, P., M. Michaelis, M. Schubert-Zsilavecz and J. Cinatl (2013) Differential antiviral and anti-inflammatory mechanisms of the flavonoids biochanin A and baicalein in H5N1 influenza A virus-infected cells. *Antiviral Res.* **97**, 41–48.
- Talia, J. M., C. E. Tonn, N. B. Debattista and N. B. Pappano (2012) Antibacterial efficacy of dihydroxylated chalcones in binary and ternary combinations with nalidixic acid and nalidix acid-rutin against *Escherichia coli* ATCC 25 922. *Indian J. Microbiol.* **52**, 638–641.
- Xie, Y.-Y., J.-L. Qu, Q.-L. Wang, Y. Wang, M. Yoshikawa and D. Yuan (2012) Comparative evaluation of cultivars of Chrysanthemum morifolium flowers by HPLC-DAD-ESI/MS analysis and antiallergic assay. *J. Agric. Food Chem.* **60**, 12574–12583.
- Navarro-Núñez, L., J. Castillo, M. L. Lozano, C. Martínez, O. Benavente-García, V. Vicente and J. Rivera (2009) Thromboxane A2 receptor antagonism by flavonoids: structure-activity relationships. *J. Agric. Food Chem.* **57**, 1589–1594.
- Khelifi, D., R. M. Sghaier, S. Amouri, D. Laouini, M. Hamdi and J. Bouajila (2013) Composition and anti-oxidant, anti-cancer and anti-inflammatory activities of *Artemisia herba-alba*, *Ruta chalapensis* L. and *Peganum harmala* L. *Food Chem. Toxicol.* **55**, 202–208.
- Martin, M. A., L. Goya and S. Ramos (2013) Potential for preventive effects of cocoa and cocoa polyphenols in cancer. *Food Chem. Toxicol.* **56**, 336–351.
- Halliwell, B. and J. M. C. Gutteridge (2007) *Free Radicals in Biology and Medicine*, 4th edn. OUP Oxford, Oxford, UK.
- Tournaire, C., S. Croux, M. T. Maurette, I. Beck, M. Hocquaux, A. M. Braun and E. Oliveros (1993) Antioxidant activity of flavonoids: Efficiency of singlet oxygen ($^1\Delta_g$) quenching. *J. Photochem. Photobiol. B Biol.* **19**, 205–215.
- Ávila, V., S. Bertolotti, S. Criado, N. Pappano, N. Debattista and N. A. García (2001) Antioxidant properties of natural flavonoids: Quenching and generation of singlet molecular oxygen. *Int. J. Food Sci. Technol.* **36**, 25–33.
- Lin, S., G. Zhang, Y. Liao, J. Pan and D. Gong (2015) Dietary flavonoids as xanthine oxidase inhibitors: structure-affinity and structure-activity relationships. *J. Agric. Food Chem.* **63**, 7784–7794.
- Santos-Buelga, C., M. T. Escribano-Bailon and V. Lattanzio (2011) *Recent Advances in Polyphenol Research*. John Wiley & Sons.
- Ferrari, G. V., N. B. Pappano, M. P. Montaña, N. A. García and N. B. Debattista (2010) Novel synthesis of 3,3'-dihydroxyflavone and apparent formation constants of flavonoid-Ga (III) complexes. *J. Chem. Eng. Data* **55**, 3080–3083.
- Montaña, M. P., N. B. Pappano and N. B. Debattista (1998) News analytical reagents for Europium (III). *Talanta* **47**, 729–733.
- Baccan, M. M., O. Chiarelli-Neto, R. M. S. Pereira and B. P. Espósito (2012) Quercetin as a shuttle for labile iron. *J. Inorg. Biochem.* **107**, 34–39.
- Bukhari, S. B., S. Memon, M. Mahroof Tahir and M. I. Bhangar (2008) Synthesis, characterization and investigation of antioxidant activity of cobalt–quercetin complex. *J. Mol. Struct.* **892**, 39–46.
- Chen, W., S. Sun, W. Cao, Y. Liang and J. Song (2009) Antioxidant property of quercetin–Cr(III) complex: The role of Cr(III) ion. *J. Mol. Struct.* **918**, 194–197.
- de Souza, R. F. V. and W. F. De Giovanni (2005) Synthesis, spectral and electrochemical properties of Al(III) and Zn(II) complexes with flavonoids. *Spectrochim. Acta. A. Mol. Biomol. Spectrosc.* **61**, 1985–90.
- Pusz, J., B. Nitka and A. Zielinska (2000) Synthesis and physico-chemical properties of the Al(III), Ga(III) and In(III) complexes with chrysin. *Microchem. J.* **65**, 245–253.
- Khan, N., D. N. Syed, N. Ahmad and H. Mukhtar (2013) Fisetin: A dietary antioxidant for health promotion. *Antioxid. Redox Signal.* **19**, 151–162.
- Kim, M. Y., L. M. Chung, D. C. Choi and H. J. Park (2009) Quantitative analysis of fustin and sulfuretin in the inner and outer heartwoods and stem bark of *Rhus verniciflua*. *Nat. Prod. Sci.* **15**, 208–212.
- Lani, R., P. Hassandarvish, M. H. Shu, W. H. Phoon, J. J. H. Chu, S. Higgs, D. Vanlandingham, S. Abu Bakar and K. Zandi (2016) Antiviral activity of selected flavonoids against Chikungunya virus. *Antiviral Res.* **133**, 50–61.
- Syed, D. N., Y. Suh, F. Afaq and H. Mukhtar (2008) Dietary agents for chemoprevention of prostate cancer. *Cancer Lett.* **265**, 167–176.
- Khan, N., F. Afaq, F. H. Khuroo, V. Mustafa Adhami, Y. Suh and H. Mukhtar (2012) Dual inhibition of phosphatidylinositol 3-kinase/Akt and mammalian target of rapamycin signaling in human non-small cell lung cancer cells by a dietary flavonoid fisetin. *Int. J. Cancer* **130**, 1695–1705.
- Ensaifi, A. A., E. Heydari-Soureshjani, M. Jafari-Asl, B. Rezaei, J. B. Ghasemi and E. Aghaee (2015) Experimental and theoretical investigation effect of flavonols antioxidants on DNA damage. *Anal. Chim. Acta* **887**, 82–91.
- Andrades Ikeda, N. E., E. M. Novak, D. A. Maria, A. S. Velosa and R. M. Silva Pereira (2015) Synthesis, characterization and biological evaluation of Rutin-zinc(II) flavonoid-metal complex. *Chem. Biol. Interact.* **239**, 184–191.
- Samsonowicz, M., E. Regulska and M. Kalinowska (2017) Hydroxyflavone metal complexes – molecular structure, antioxidant activity and biological effects. *Chem. Biol. Interact.* **273**, 245–256.
- Zhang, L., Y. Liu, Y. Wang, M. Xu and X. Hu (2018) UV-Vis spectroscopy combined with chemometric study on the interactions of three dietary flavonoids with copper ions. *Food Chem.* **263**, 208–215.
- Dimitrić Marković, J. M., Z. S. Marković, D. S. Veselinović, J. B. Krstić and J. D. Predojević Simović (2009) Study on fisetin-aluminum(III) interaction in aqueous buffered solutions by spectroscopy and molecular modeling. *J. Inorg. Biochem.* **103**, 723–730.
- Liu, Y. and M. Guo (2015) Studies on transition metal-quercetin complexes using electrospray ionization tandem mass spectrometry. *Molecules* **20**, 8583–8594.
- Esmaeili, L., M. G. Perez, M. Jafari, J. Paquin, P. Ispas-Szabo, V. Pop, M. Andruh, J. Byers and M. A. Mateescu (2019) Copper complexes for biomedical applications: Structural insights, antioxidant activity and neuron compatibility. *J. Inorg. Biochem.* **192**, 87–97.
- Bonnett, R. (1995) Photosensitizers of the porphyrin and phthalocyanine series for photodynamic therapy. *Chem. Soc. Rev.* **24**, 19–33.

33. Rizzi, V., P. Fini, F. Fanelli, T. Placido, P. Semeraro, T. Sibillano, A. Fraix, S. Sortino, A. Agostiano, C. Giannini and P. Cosma (2016) Molecular interactions, characterization and photoactivity of Chlorophyll *a*/chitosan/2-HP- β -cyclodextrin composite films as functional and active surfaces for ROS production. *Food Hydrocoll.* **58**, 98–112.
34. Suzuki, M., M. Endo, F. Shinohara, S. Echigo and H. Rikiishi (2011) Rapamycin suppresses ROS-dependent apoptosis caused by selenomethionine in A549 lung carcinoma cells. *Cancer Chemother. Pharmacol.* **67**, 1129–1136.
35. Wilkinson, F., W. P. Helman and A. B. Ross (1995) Rate constants for the decay and reactions of the lowest electronically excited singlet state of molecular oxygen in solution. An expanded and revised Compuation. *J. Phys. Chem. Ref. Data* **24**, 663–677.
36. Pękal, A., M. Biesaga and K. Pyrzynska (2011) Interaction of quercetin with copper ions: complexation, oxidation and reactivity towards radicals. *Biomaterials* **24**, 41–49.
37. Muñoz, V. A., G. V. Ferrari, M. I. Sancho and M. P. Montaña (2016) Spectroscopic and thermodynamic study of chrysin and quercetin complexes with Cu(II). *J. Chem. Eng. Data* **61**, 987–995.
38. Sawyer, D. T., W. R. Heinman and J. M. Beebe (1984) *Chemistry Experiments for Instrumental Methods*. John Wiley & Sons, New York.
39. Harris, D. C. (1991) *Análisis Químico Cuantitativo*, 3rd edn. Grupo Editorial Iberoamérica, México D.F.
40. Becke, A. D. (1988) Density-functional exchange-energy approximation with correct asymptotic behavior. *Phys Rev A Gen Phys* **38**, 3098–3100.
41. Lee, C., W. Yang and R. G. Parr (1988) Development of the Colle-Salvetti correlation-energy formula into a functional of the electron density. *Phys. Rev. B* **37**, 785–789.
42. Cancès, E., B. Mennucci and J. Tomasi (1997) A new integral equation formalism for the polarizable continuum model: Theoretical background and applications to isotropic and anisotropic dielectrics. *J. Chem. Phys.* **107**, 3032.
43. Stratmann, R. E., G. E. Scuseria and M. J. Frisch (1998) An efficient implementation of time-dependent density-functional theory for the calculation of excitation energies of large molecules. *J. Chem. Phys.* **109**, 8218–8224.
44. Adamo, C. and V. Barone (1999) Toward reliable density functional methods without adjustable parameters: The PBE0 model. *J. Chem. Phys.* **110**, 6158–61570.
45. Ernzerhof, M. and G. E. Scuseria (1999) Assessment of the Perdew-Burke-Ernzerhof exchange-correlation functional. *J. Chem. Phys.* **110**, 5029–5036.
46. Zhao, Y. and D. G. Truhlar (2008) The M06 suite of density functionals for main group thermochemistry, thermochemical kinetics, noncovalent interactions, excited states, and transition elements: Two new functionals and systematic testing of four M06-class functionals and 12 other function. *Theor. Chem. Acc.* **120**, 215–241.
47. Yanai, T., D. P. Tew and N. C. Handy (2004) A new hybrid exchange-correlation functional using the Coulomb-attenuating method (CAM-B3LYP). *Chem. Phys. Lett.* **393**, 51–57.
48. Martin, R. L. (2003) Natural transition orbitals. *J. Chem. Phys.* **118**, 4775–4777.
49. Frisch, M. J., G. W. Trucks, H. B. Schlegel, G. E. Scuseria, M. A. Robb, J. R. Cheeseman, G. Scalmani, V. Barone, B. Mennucci, G. A. Petersson, H. Nakatsuji, M. Caricato, X. Li, H. P. Hratchian, A. F. Izmaylov, J. Bloino, G. Zheng and D. J. F. Sonnenb (2013) Gaussian 09. 2013.
50. Scully, F. E. and J. Hoigné (1987) Rate constants for reactions of singlet oxygen with phenols and other compounds in water. *Chemosphere* **16**, 681–694.
51. Bertolotti, S. G., C. M. Previtali, A. M. Rufs and M. V. Encinas (1999) Riboflavin/triethanolamine as photoinitiator system of vinyl polymerization. A mechanistic study by laser flash photolysis. *Macromolecules* **32**, 2920–2924.
52. Neumann, M. and N. A. García (1992) Kinetics and mechanism of the light-induced deterioration of lemon oil. *J. Agric. Food Chem.* **40**, 957–960.
53. Criado, S. and Garcia, N. A. (2004) Vitamin B2- sensitized photooxidation of the ophthalmic drugs Timolol and Pindolol: kinetics and mechanism. *Redox Rep.* **9**, 291–297.
54. Heelis, P. F. (1982) The photophysical and photochemical properties of flavins (isoalloxazines). *Chem. Soc. Rev.* **11**, 15–39.
55. Escalada, J. P., A. Pajares, J. Gianotti, W. A. Massad, S. Bertolotti, F. Amat-Guerri and N. A. García (2006) Dye-sensitized photodegradation of the fungicide carbendazim and related benzimidazoles. *Chemosphere* **65**, 237–244.
56. Silva, E., L. Herrera, A. M. Edwards, J. De La Fuente and E. Lissi (2005) Enhancement of riboflavin mediated photooxidation of glucose-6-phosphate-dehydrogenase by urocanic acid. *Photochem. Photobiol.* **81**, 206–211.
57. Silva, E., A. M. Edwards and D. Pacheco (1999) Visible light-induced photooxidation of glucose sensitized by riboflavin. *J. Nutr. Biochem.* **10**, 181–185.
58. Łodyga-Chruscińska, E., M. Pilo, A. Zucca, E. Garribba, E. Klewicka, M. Rowińska-Żyrek, M. Symonowicz, L. Chrusciński and V. T. Cheshechik (2018) Physicochemical, antioxidant, DNA cleaving properties and antimicrobial activity of fisetin-copper chelates. *J. Inorg. Biochem.* **180**, 101–118.
59. Jabeen, E., N. K. Janjua, S. Ahmed, I. Murtaza, T. Ali, N. Masood, A. S. Rizvi and G. Murtaza (2017) DFT predictions, synthesis, stoichiometric structures and anti-diabetic activity of Cu (II) and Fe (III) complexes of quercetin, morin, and primuletin. *J. Mol. Struct.* **1150**, 459–468.
60. Ma, L., J. Koka, A. J. Stace and H. Cox (2014) Gas phase UV spectrum of a Cu(II)-bis(benzene) sandwich complex: Experiment and theory. *J. Phys. Chem. A* **118**, 10730–10737.
61. Hanuza, J., P. Godlewska, E. Kucharska, M. Ptak, M. Kopacz, M. Mączka, K. Hermanowicz and L. Macalik (2017) Molecular structure and vibrational spectra of quercetin and quercetin-5'-sulfonic acid. *Vib. Spectrosc.* **88**, 94–105.
62. Montaña, M. P., W. A. Massad, S. Criado, A. Biasutti and N. A. García (2010) Stability of flavonoids in the presence of riboflavin-photogenerated reactive oxygen species: A kinetic and mechanistic study on quercetin, morin and rutin. *Photochem. Photobiol.* **86**, 827–834.
63. Krishna, C. M., U. Shobha, P. Riesz, J. S. Jr Zigler and D. Balasubramanian (1991) A study of the photodynamic efficiencies of some eye lens constituents. *Photochem. Photobiol.* **54**, 51–58.
64. Wilkinson, F., P. Helman and A. B. Ross (1993) Quantum yields for the photosensitized formation of the lowest electronically excited singlet state of molecular oxygen in solution quantum yields for the photosensitized formation of the lowest electronically excited singlet state of molecular oxygen in. *J. Phys. Chem. Ref. Data* **22**, 113–262.
65. Muñoz, V. A., G. V. Ferrari, M. P. Montaña, S. Miskoski and N. A. García (2016) Effect of Cu²⁺-complexation on the scavenging ability of chrysin towards photogenerated singlet molecular oxygen ($O_2(^1\Delta_g)$). Possible biological implications. *J. Photochem. Photobiol. B Biol.* **162**, 597–603.
66. Ferrari, G. V., M. P. Montaña, F. C. D. Dimarco, N. B. Debattista, N. B. Pappano, W. A. Massad and N. A. García (2013) A comparative photochemical study on the behavior of 3,3'-dihydroxyflavone and its complex with La(III) as generators and quenchers of reactive oxygen species. *J. Photochem. Photobiol. B Biol.* **124**, 42–49.
67. Varnes, A. W., R. B. Dodson and E. L. Wehry (1972) Interactions of transition-metal ions with photoexcited states of flavins. Fluorescence quenching studies. *J. Am. Chem. Soc.* **94**, 946–950.
68. Baynes, J. W. and M. H. Dominiczak (2005) *Bioquímica Médica*. Elsevier, España.
69. Görner, H. (2007) Oxygen uptake after electron transfer from amines, amino acids and ascorbic acid to triplet flavins in air-saturated aqueous solution. *J. Photochem. Photobiol. B Biol.* **87**, 73–80.
70. Bertolotti, S. G., N. A. García and G. A. Argüello (1991) Effect of the peptide bond on the singlet-molecular-oxygen-mediated sensitized photo-oxidation of tyrosine and tryptophan dipeptides. A kinetic study. *J. Photochem. Photobiol. B Biol.* **10**, 57–70.